WWW.IJRPR.COM

International Journal of Research Publication and Reviews

Journal homepage: www.ijrpr.com ISSN 2582-7421

Selecting Numerical Turbulence Model of Car Spoiler by Using Statist Method and Comparing to Theoretical Data

Luigi Buffone [(a)]

[a] *Department of Mechanical Engineering, Slovak University of technology in Bratislava (STU), Bratislava, Slovak*
DOI: https://doi.org/10.55248/gengpi.4.623.45049

A B S T R A C T

The turbulent model selection was carried out on a three-dimensional wing profile, NACA model, with pronounced camber for automotive applications. The analysis was conducted for five turbulent models [Spalart-Allmaras, SST k-Omega, k-kL-Omega, Transient SST, and Reynolds Stress] at various angles of attack ranging from 0 to 45 degrees, with a velocity of 50 m/s. To perform the analysis, Ansys Fluent solver was used under steady-state conditions with a tetrahedral mesh geometry consisting of 444,623 cells, determined based on sensitivity analysis, where grid refinement is near the wing profile to accurately represent the boundary layer. A steady flow analysis was chosen, varying the angle of attack to compare the results with those provided by the National Advisory Committee for Aeronautics (NACA). The selection of the turbulent model was made using a statistical approach that highlights the model that best approximates the mean values of drag and lift forces

Keywords: Computational fluid dynamics (CFD), airfoil, spoiler, aerodynamic forces, lift, drag, turbulence models.

Introduction

The design of industrial components in the automotive, aerospace, chemical, and mechanical sectors has heavily relied on Computer-Aided Engineering (CAE) packages over the past decade and they consist of various dedicated software tools such as Computer-Aided Design (CAD) for geometric modeling, Computational Fluid Dynamics (CFD), and Finite Element Method (FEM) for fluid dynamics and mechanical analysis of components. The accuracy of the obtained results primarily depends on the mesh used near the area of interest, the chosen parameters for the desired simulation, and the mathematical model adopted.

The most time-consuming and computationally demanding simulations are typically transient-state simulations, which involve long waiting times for the results, depending on the computational power available. In the case of the examined spoiler, the chaotic motion around the wing profile was analyzed to evaluate the most suitable turbulent model for the spoiler. This analysis involved varying the turbulent model, starting from the simpler single-equation Spalart-Allmaras model to the more complex 5-equation SST Reynolds stress model, in order to determine which one was most appropriate for the specific spoiler being studied.

The type of fluid flow affecting the spoiler is an external flow that forms two boundary layers on its surfaces: one on the upper side and one on the lower side with a pressure difference between these layers, pushing the wing profile downward and generating downforce (negative lift force).

Nomenclature

ρair density
$t$time
u velocity in x-direction
v velocity in y-direction
w velocity in z-direction
V velocity
$\tilde{u}$ average velocity
u'velocity fluctuation
p air pressure
v air viscosity
G_v turbulence model coefficient
$Y_v$turbulence model coefficient
$\sigma_{\tilde{v}}$ turbulence model coefficient
C_{b2}turbulence model coefficient
Γ turbulent diffusion of heat or mass
μ effective dynamic viscosity
μ_t turbulent dynamic viscosity
$\tilde{v}$ molecular kinematic viscosity
k turbulent kinetic energy
C_{b1} turbulence model coefficient
C_{b2} turbulence model coefficient
C_{v1} turbulence model coefficient
C_{w2} turbulence model coefficient
C_{w3} turbulence model coefficient
D_ω turbulence model coefficient
S_k turbulence model coefficient
ε rate of dissipation of the turb. kin. energy,
$\alpha_\varepsilon$inverse value for turbulent Prandtl number for

Mathematical Equations

The fundamental equation is that of continuity, where the mass of fluid entering the domain is equal to the mass exiting the domain, resulting in a variation of zero. This equation is expressed as follows:

$$\frac{\partial \rho}{\partial t} + \frac{\partial (\rho u)}{\partial x} + \frac{\partial (\rho v)}{\partial y} + \frac{\partial (\rho w)}{\partial z} = 0 \qquad (1)$$

The second fundamental equation is the conservation of momentum, referring to an inertial system which in the case of a 3D model is represented by three equations along the three respective axes and can be expressed as follows:

$$\frac{\partial V_i}{\partial t} + V_i \frac{\partial V_i}{\partial x_j} = -\frac{1}{\rho}\frac{\partial p}{\partial x_i} + \nu \frac{\partial^2 V_i}{\partial x_i \partial x_j} \qquad (2)$$

The single-equation turbulent model represented by Spalart-Allmaras is suitable for flows with low velocities, where the turbulent kinetic viscosity is solved using the following equation:

$$\frac{\partial}{\partial t}(\rho \tilde{v}) + \frac{\partial}{\partial x_i}(\rho \tilde{v} u_i) = G_v \frac{1}{\sigma_{\tilde{v}}}\left\{\frac{\partial}{\partial x_i}\left[(\mu + \rho \tilde{v})\frac{\partial \tilde{v}}{\partial x_i}\right] + C_{b2}\rho\left(\frac{\partial \tilde{v}}{\partial x_i}\right)^2\right\} - Y_v + S_{\tilde{v}} \qquad (3)$$

The turbulent model (SST) K-Omega utilizes two equations to describe the turbulent portion, one equation resolves turbulence near the surfaces of the spoiler, while the other equation is dedicated to turbulent motion that develops away from the rigid walls. These equations are as follows:

$$\frac{\partial}{\partial t}(\rho k) + \frac{\partial}{\partial x_i}(\rho k u_i) = \frac{\partial}{\partial x_j}\left(\Gamma_k \frac{\partial k}{\partial x_j}\right) + \tilde{G}_k - Y_k + S_k \qquad i,j=1,3 \qquad (4)$$

$$\frac{\partial}{\partial t}(\rho \omega) + \frac{\partial}{\partial x_i}(\rho \omega u_i) = \frac{\partial}{\partial x_j}\left(\Gamma_\omega \frac{\partial \omega}{\partial x_j}\right) + G_\omega - Y_\omega + D_\omega + S_\omega \qquad i,j=1,3 \qquad (5)$$

Another more complex model compared to the previous one is called k-kL-Omega which consists of three equations dedicated to resolving the chaotic motion and in addition to the (SST) K-Omega model, it includes an additional equation that better captures the transition turbulence between the region near the surfaces of the spoiler and the region further away. This additional equation generates a more uniform description at different distances from the walls. The equation is as follows:

$$\frac{Dk_T}{Dt} = P_{k_T} + R + R_{NAT} - \omega k_T - D_T + \frac{\partial}{\partial x_j}\left[\left(\nu + \frac{\alpha_T}{\alpha_K}\right)\frac{\partial k_T}{\partial x_j}\right] \qquad (6)$$

$$\frac{Dk_L}{Dt} = P_{k_L} - R - R_{NAT} - D_L + \frac{\partial}{\partial x_j}\left(\nu \frac{\partial k_L}{\partial x_j}\right) \qquad (7)$$

$$\frac{D\omega}{Dt} = C_{\omega 1}\frac{\omega}{k_T}P_{K_T} + \left(\frac{C_{wR}}{f_w} - 1\right)\frac{\omega}{k_T}(R + R_{NAT}) - C_{\omega_2}\omega^2 + C_{\omega_3} f_w \alpha_T f_w{}^2 \frac{\sqrt{k_T}}{d^3} + \frac{\partial}{\partial x_j}\left[\left(\nu + \frac{\alpha_T}{\alpha_\omega}\right)\frac{\partial \omega}{\partial x_j}\right] \qquad (8)$$

The SST Transient turbulent model is an extension of the SST k-Omega model, where, in addition to the two classic equations from the previous model, there is an additional transport equation. This allows for a turbulent model consisting of a total of three equations.

$$\frac{\partial}{\partial t}(\rho \gamma) + \frac{\partial}{\partial x_j}(\rho \gamma u_j) = P_{\gamma 1} - E_{\gamma 1} + P_{\gamma 2} - E_{\gamma 2} + \frac{\partial}{\partial x_j}\left[\left(\mu \frac{\mu_t}{\sigma_\gamma}\right)\frac{\partial \gamma}{\partial x_j}\right] \qquad i,j=1,3 \qquad (9)$$

$$\frac{\partial}{\partial t}(\rho k) + \frac{\partial}{\partial x_j}(\rho u_j k) = \tilde{P}_k - \tilde{D}_k + \frac{\partial}{\partial x_j}\left[(\mu + \sigma_k \mu_t)\frac{\partial k}{\partial x_j}\right] \qquad i,j=1,3 \qquad (10)$$

One of the most complex numerical models is represented by the Reynolds Stress Model (RSM), which describes turbulent motion using five different equations with high-level information and it is well suited for complex spoiler geometries that have pronounced curvature. The RSM model is primarily used in cases involving rotating vortices of varying sizes within the flow:

$$\frac{\partial}{\partial t}(\rho \overline{u_i{}' u_j{}'}) + \frac{\partial}{\partial x_k}(\rho u_k \overline{u_i{}' u_j{}'}) = -\frac{\partial}{\partial x_k}\left[\rho \overline{u_i{}' u_j{}' u_k{}'} + p(\overline{\delta_{kj} u_i{}'} + \overline{\delta_{ki} u_j{}'})\right]$$
$$+ \frac{\partial}{\partial x_k}\left[\mu \frac{\partial}{\partial x_k}\overline{u_i{}' u_j{}'}\right] - \rho\left(\overline{u_i{}' u_k{}'}\frac{\partial u_j}{\partial x_k} + \overline{u_j{}' u_k{}'}\frac{\partial u_i}{\partial x_k}\right) - \rho\beta\left(g_i \overline{u_j{}'\theta} + g_i \overline{u_i{}'\theta}\right)$$
$$+ p\left(\overline{\frac{\partial u_i{}'}{\partial x_j}} + \overline{\frac{\partial u_i{}'}{\partial x_i}}\right) - 2\mu\left(\overline{\frac{\partial u_i{}'}{\partial x_k}\frac{\partial u_j{}'}{\partial x_k}}\right) - 2\rho\Omega_k\left(\overline{u_j{}' u_k{}'}\varepsilon_{ikm} + \overline{u_i{}' u_m{}'}\varepsilon_{jkm}\right) + S_{user} \qquad i,j=1,3 \qquad (11)$$

CFD Method

The chosen wing profile for the spoiler was the NACA 6409, which has a thickness equal to 60% of the chord length, with a position located at 40% of the chord length from the leading edge. A high-camber aerodynamic profile was selected to ensure high lift force at low velocities, making it suitable for automotive applications (fig. 1).

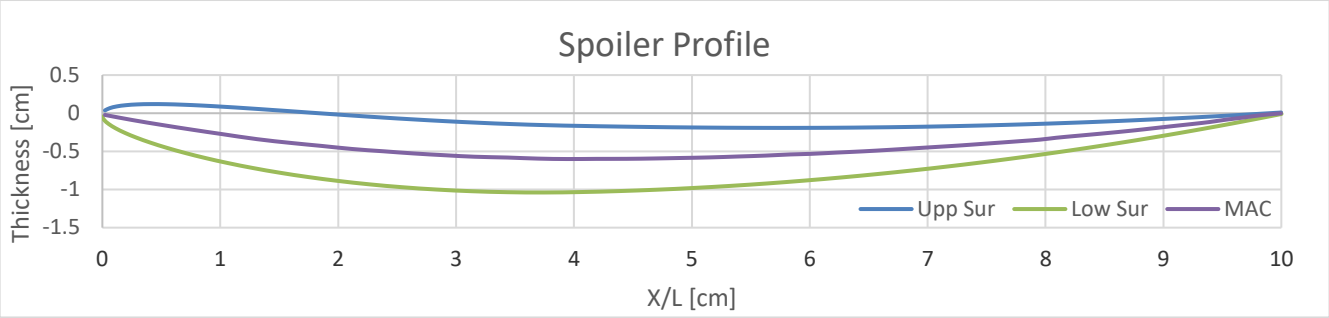

Figure 1 Spoiler 2D Geometry

The first step involved constructing the spoiler's geometry in CAD by utilizing the coordinates of the points and then joining and extruding them to obtain the 3D model. After creating the spoiler, the next task was to define the dimensions of the domain in the space surrounding the profile to delimit the region relevant to the fluid flow, which extends in front, above, and below the model for a length equal to 30 times the chord length, meanwhile the rear part, which is influenced by turbulence, had a larger extension
with a length of 0.35 meters. To facilitate easy rotation of the spoiler and reduce mesh regeneration time for new simulations, a cylinder was created around the spoiler (Fig. 2).

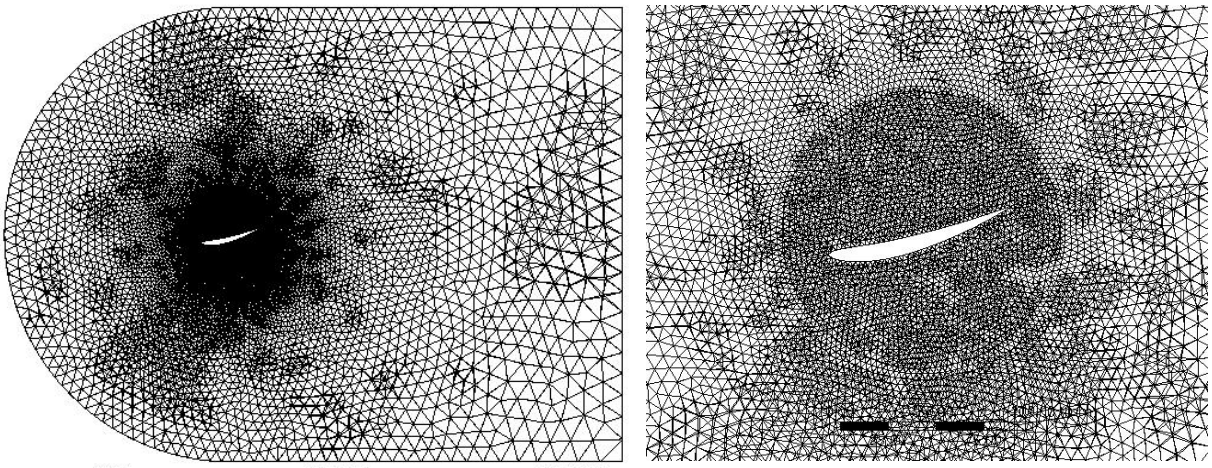

Figure 2 Mesh domain (a) mesh around spoiler (b) zoomed mesh

The fluid has an inlet velocity of 50 m/s and an outlet pressure of 0 Pa. The angle of attack is 0, 5, 10, 15, 20, 25, 30, 40, 45 degree under steady flow conditions. The top, bottom, and right surfaces are set as walls, while the left surface represents a symmetry surface. The density of the air is 1.175 kg/m^3, and the viscosity is $\mu = 1.7894 \times 10^{-5}$ kg/(m·s) and the turbulence intensity is 10%. The flow is considered incompressible, as the Reynolds number is low and equal to 330,885.

A tetrahedral mesh was used, which ensures stability of cell angles with low distortion, and refinement was done near the surfaces of the spoiler. The dependency of the mesh on the results was investigated using the sensitivity method, with the lift forces and pitching moment chosen as the output parameters.
An refinement was adopted with a total of 444,623 cells, where the variation in the results dropped below 0.60%, indicating a low deviation from the desired accuracy (Tab. 1).

Cells	**Lift Force**	**Pitching Moment**	**Lift Variation**	**Pitch Variation**
67,789	-12.1590032	-0.34091025	0.0000%	0.0000%
105,193	-11.647292	-0.3200707	4.3934%	6.5109%
181,334	-11.536885	-0.31679212	0.9479%	1.0243%

272,220	-11.440481	-0.31408983	0.8356%	0.8530%
444,623	-11.3775892	-0.31225623	0.5497%	0.5838%

Table 1 CFD Mesh Independency Study

The mesh used is considered fine, with a minimum orthogonal quality of 0.6877738 and the smallest aspect ratio of 1.1575. The maximum orthogonal quality is 0.9843364, and the maximum aspect ratio is 13.917.

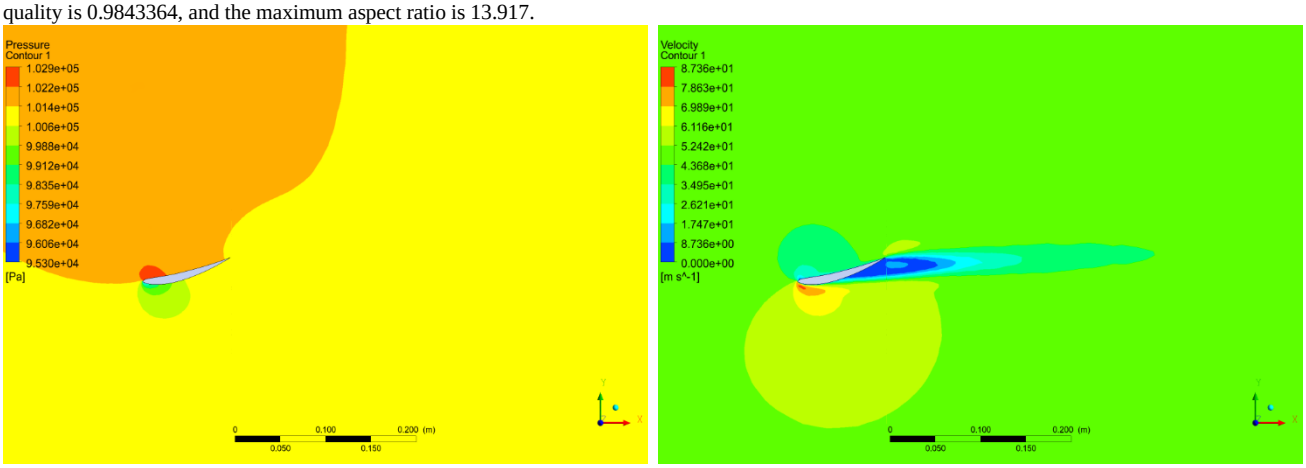

Figure 3 Spalart-Allmaras Model Results (a) Pressure Contour (b) Velocity Contour

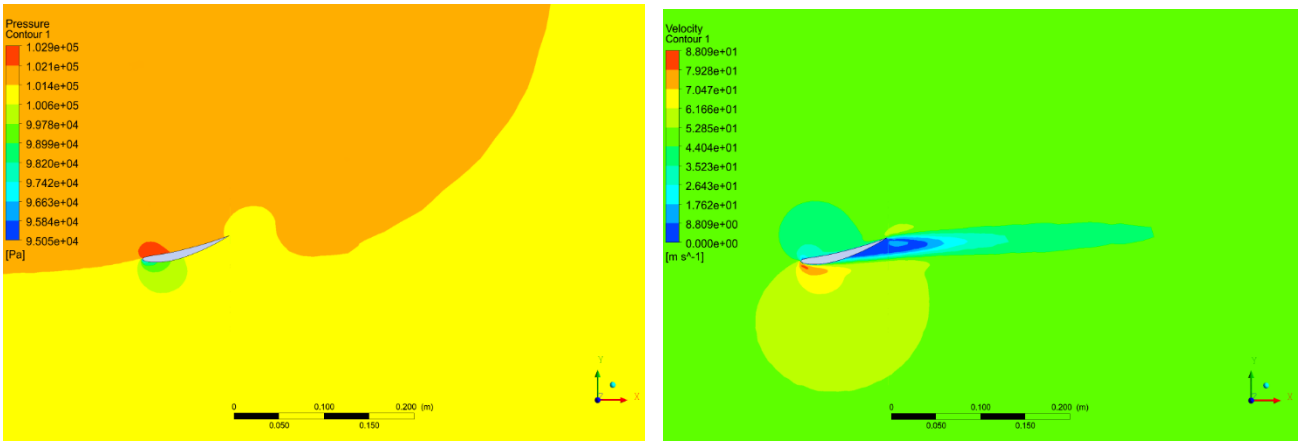

Figure 4 k-Omega Model Results (a) Pressure Contour (b) Velocity Contour

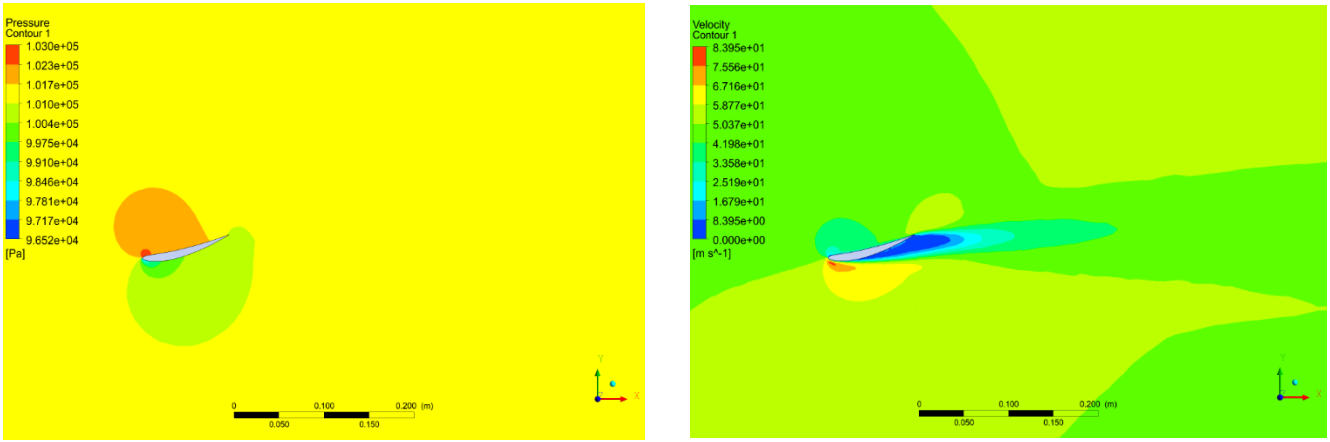

Figure 5 k-kl-Omega Model Results (a) Pressure Contour (b) Velocity Contour

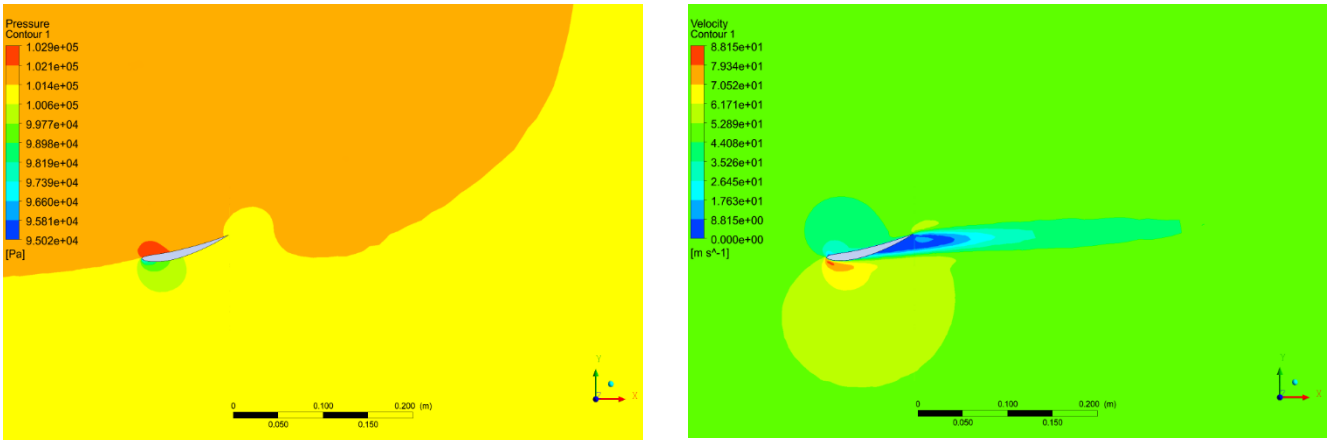

Figure 6 Transient SST Model Results (a) Pressure Contour (b) Velocity Contour

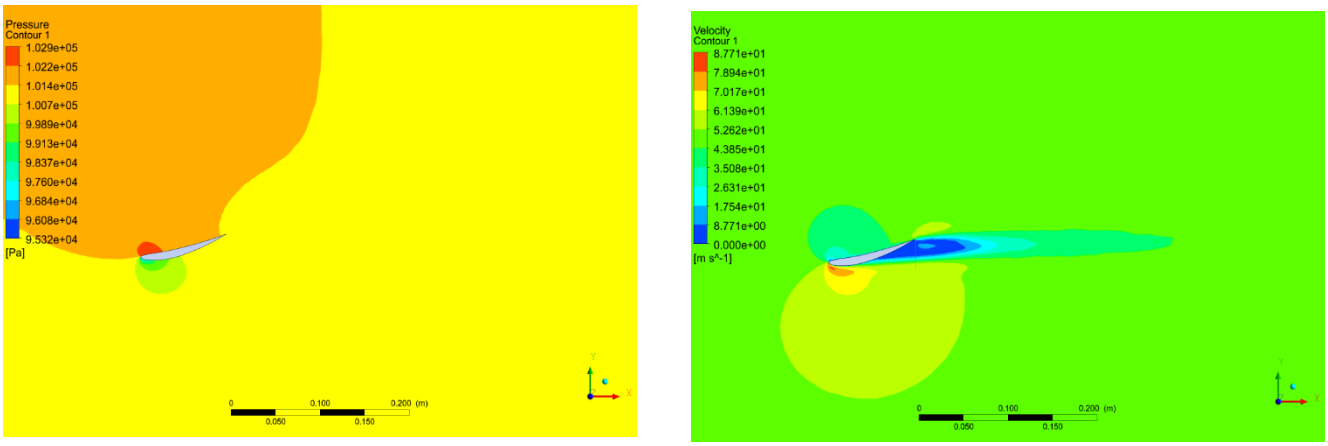

Figure 7 Reynolds Stress Model Results (a) Pressure Contour (b) Velocity Contour

Comparison Data

The lift and drag curves were compared to those provided by NASA at different angles of attack, three different speeds, and with angles of attack ranging from a minimum of -10 to +20 degrees for lift. Regarding the drag coefficient, angles ranging from 0 to +20 degrees were used. The difference in the angles of the two curves is primarily due to the variation in aspect ratio. In the case of the NASA data, the profile has a 2D geometry with an infinite aspect ratio, while the profile used in the fluid dynamics simulation has an aspect ratio of 4. The stall of the 2D profile occurs at an angle of attack of 11.75 degrees, whereas the 3D profile stalls at 15 degrees. As for the drag coefficient, it is higher in the case of the 3D geometry spoiler.

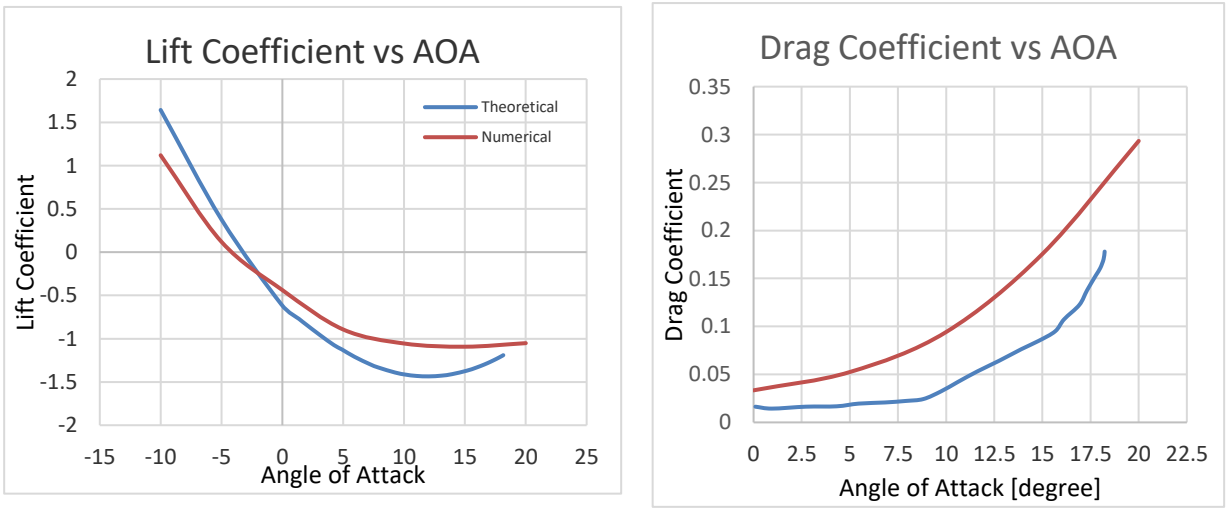

Figure 8 Blue Infinite AR and Red 4 AR (a) Lift curves (b) Drag curves

Results and Discussion

From the comparative analysis of the average data with the median data, the latter approach the turbulent model SST K-Omega, which consists of a double equation.

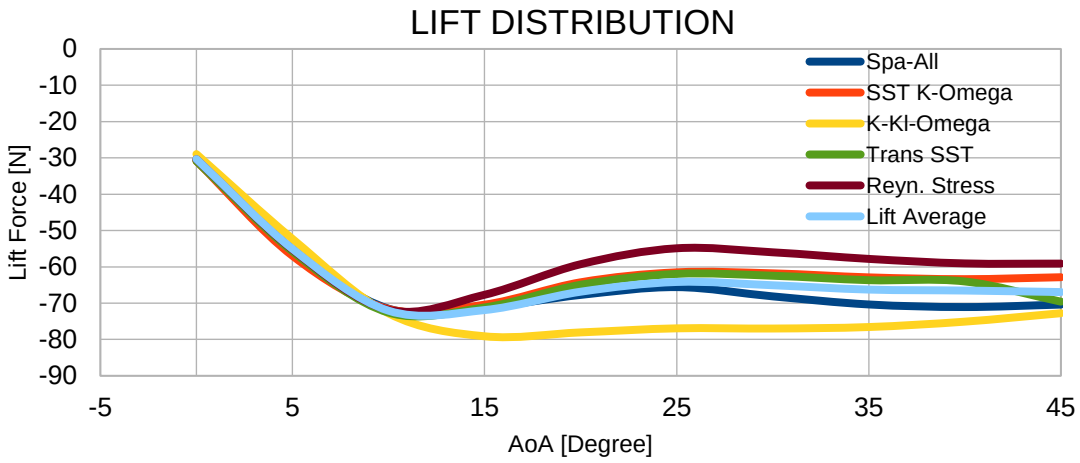

Figure 9 Lift Force variation versus turbulent model

AoA	Spa-All	SST K-Omega	K-Kl-Omega	Trans SST	Reyn. Stress	Lift Average
0	-30.576919	-30.845597	-28.94917	-30.871647	-30.354971	-30.3196608
5	-55.102478	-56.965421	-52.311498	-55.752367	-55.241386	-55.07463
10	-71.511883	-71.610924	-72.814721	-72.585382	-71.836783	-72.0719386
15	-71.126961	-70.418383	-79.125925	-71.179994	-67.685852	-71.907423
20	-67.732087	-64.260204	-78.055013	-64.942843	-59.27623	-66.8532754
25	-65.585979	-61.506533	-76.937591	-61.941324	-54.887307	-64.1717468
30	-68.135177	-61.789517	-76.987029	-62.453714	-55.997062	-65.0724998
35	-70.361684	-62.896754	-76.575828	-63.674702	-57.811407	-66.264075
40	-71.073305	-63.386486	-75.094864	-64.02738	-59.058845	-66.528176
45	-70.395971	-62.860072	-72.768327	-69.587104	-59.105708	-66.9434364
AVERAGE	**-64.1602444**	**-60.6539891**	**-68.9619966**	**-61.7016457**	**-57.1255551**	**-62.52068618**

Table 2 Lift Force variation versus turbulent model

From the analysis of the lift force results, the curves of the various turbulent models exhibit a division into two parts, regarding values below the stall point, the curves are concentrated in the same region, while for angles of attack greater than the stall point, the curves show a more widespread distribution. The two curves that deviate the most from the mean value are the k-kL-Omega model and the Reynolds stress model, in contrast to the Spart-Allamarat, SST K-Omega, and Transient SST models. As the angle of attack increases above the stall point, lift increases non-linearly for angles of attack ranging from 10 to 25 degrees, and then stabilizes for almost all turbulent models, except for the Reynolds Stress model (fig. 9).

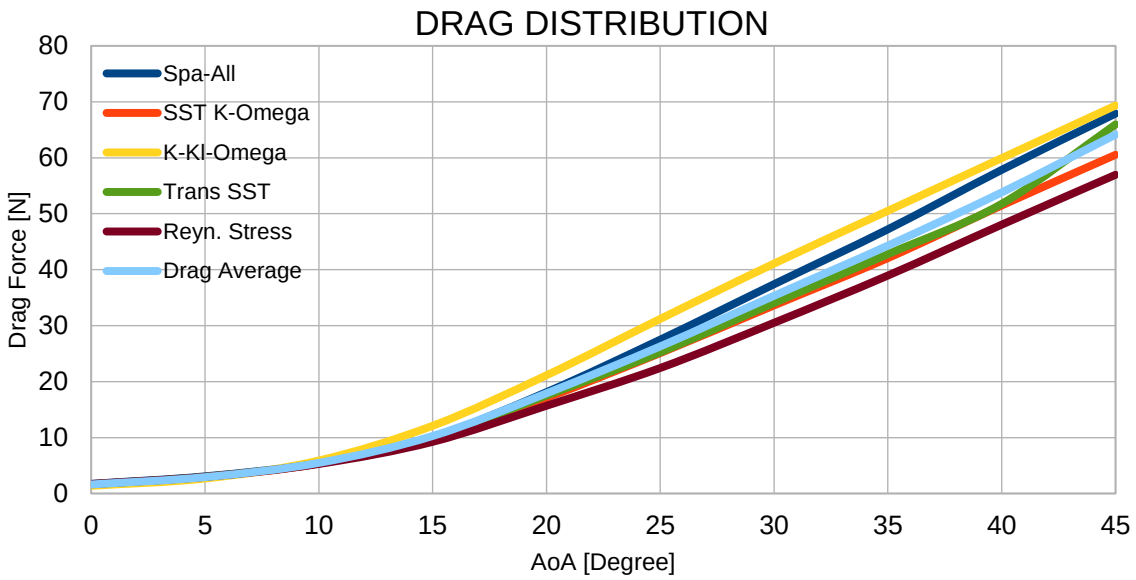

Figure 10 Drag Force variation versus turbulent model

AoA	Spa-Allmarat	SST K-Omega	K-Kl-Omega	Transient SST	Reynold Stress	Drag Average
0	1.726678	1.6393066	1.3786308	1.6375429	1.6934675	1.61512516
5	3.0630847	2.9021737	2.6838344	2.9872396	2.9769842	2.92266332
10	5.450576	5.3479883	5.8893176	5.3926893	5.2828255	5.47267934
15	10.082644	9.9586059	12.102151	10.003129	9.236178	10.27654158
20	18.112443	17.076474	21.125792	17.507325	15.682254	17.9008576
25	27.496034	25.09782	31.208527	25.231235	22.43163	26.2930492
30	37.404564	33.616902	41.093349	34.049885	30.514124	35.3357648
35	47.218636	42.067254	50.517392	42.772214	38.953269	44.305753
40	57.840003	51.473208	59.934411	51.767947	48.044006	53.811915
45	67.896781	60.52722	69.335035	65.953087	56.958996	64.1342238
AVERAGE	**27.62914437**	**24.97069525**	**29.52684398**	**25.73022938**	**23.17737342**	**26.20685728**

Table 3 Lift Force variation versus turbulent model

The behavior of drag force, unlike lift, is different because all turbulent models for low angles of attack give coinciding results, indicating that the model does not influence the value of drag. In the case of increasing angles of attack from a minimum of 12.5 degrees to a maximum of 45 degrees, turbulent models vary linearly and remain within a restricted range. An exception is the Transient SST model, which for angles of attack greater than 32.5 degrees does not follow the linear trend like the others (Fig. 10).

The total force exhibits a trend similar to that of lift since lift is the dominant force compared to drag, as the spoiler has a much larger surface area in the direction of this force. For angles below 10 degrees, turbulent models cluster around an area near the average curve, while for larger angles, the trend expands, just like in the case of lift. For almost all models, they follow the average trend (constant trend), except for the Transient SST model, which diverges from the mean value for angles greater than 45 degrees (Fig. 11). The turbulent models that are positioned further away from the mean value are Reynolds Stress and K-Kl-Omega, while the model closest to the mean value is the SST k-ω model, which is the most suitable model for low Reynolds numbers and external flows, such as the spoiler or other types of airfoil profiles.

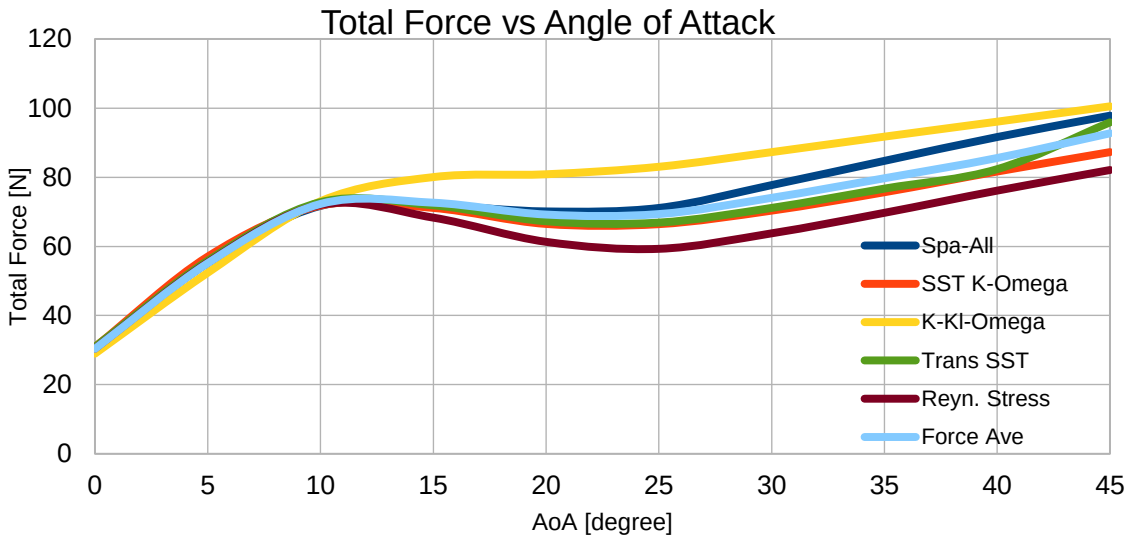

Figure 11 Total Force variation versus turbulent model

AoA	Spa-All	SST K-Omega	K-Kl-Omega	Transient SST	Reyn. Stress	Force Ave
0	30.62563293	30.88912722	28.98197831	30.91504707	30.40217256	30.36279162
5	55.18754905	57.0393005	52.38029964	55.83233854	55.32154338	55.15220622
10	71.71930137	71.81034337	73.05249931	72.78542971	72.03076868	72.27966849
15	71.83804209	71.11907266	80.04607464	71.87944168	68.313114	72.63914901
20	70.11202608	66.49044881	80.86336712	67.26127627	61.31561411	69.20854648
25	71.11647156	66.43006978	83.02629142	66.88305345	59.29413541	69.35000432
30	77.7271108	70.34230954	87.26778309	71.13270036	63.77133146	74.04824705
35	84.73704126	75.66806144	91.73802008	76.70677913	69.71022841	79.71202607
40	91.63449476	81.65376751	96.08003029	82.33726815	76.13260593	85.56763333
45	97.80370956	87.26358354	100.5115739	95.87582974	82.08417596	92.70777455
AVERAGE	**72.25013794**	**67.87060844**	**77.39479178**	**69.16091641**	**63.83756899**	**70.10280471**

Table 4 Total Force variation versus turbulent model

The statistical average of the drag and lift forces results was calculated in order to analyse the turbulent model that best approximates them and to be adopted as the most significant turbulent model for the analysed spoiler. The process was carried out in steps, keeping all values constant and varying only the angle of attack in order to collect a series of results that were similar. The distribution of the results follows a Gaussian distribution with a bell-shaped curve, where the probability increases at the center and gradually decreases as you move away from the median value. The normal distribution has a bell-shaped curve with its peak in the center, while the distribution depicted in Fig. 12 has an inverted shape because it has been analyzed for the downforce, which represents negative lift. For low angles of attack ranging from 0 to 15 degrees, the distribution appears concentrated, with a more pronounced frequency at the center since this is the range where the profile does not experience stall. For higher angles of attack, the turbulence downstream of the spoiler increases, and the distribution becomes flatter with a low variation in frequency.

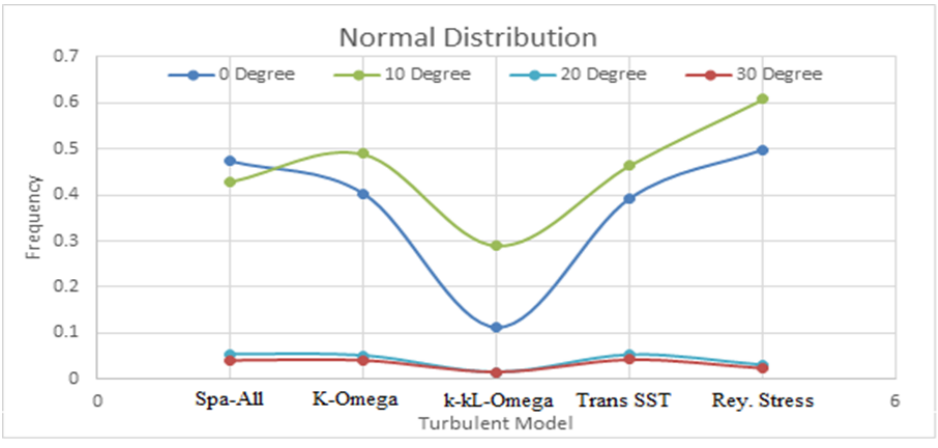

Figure 12 Turbulent models distribution

AoA\Statist.	Force Ave	Median	Std Dev	Skewness	Kurtosis
0 degree	30.36279162	30.6256329	0.79989016	-1.87272863	3.633077014
5 degree	55.15220622	55.3215434	1.7129722	-1.18195567	2.443144333
10 degree	72.27966849	72.0307687	0.60193239	0.56588823	-2.54288914
15 degree	72.63914901	71.8380421	4.39052064	1.580017013	3.323696782
20 degree	69.20854648	67.2612763	7.24792069	1.165118349	2.147045514
25 degree	69.35000432	66.8830534	8.74490708	0.938795345	1.688716767
30 degree	74.04824705	71.1327004	8.89015679	0.710961892	0.432360386
35 degree	79.71202607	76.7067791	8.59209557	0.507330792	-0.68117719
40 degree	85.56763333	82.3372681	8.09460692	0.354670574	-1.64248316
45 degree	92.70777455	95.8758297	7.73635047	-0.64878338	-1.68401555
Average	**70.10280471**	**69.1609164**	**5.07215802**	**0.446234974**	**0.338269301**

Table 5 Percentage Deviation of Average Turbulence Models

The median approaches the mean force, which is determined by the combined lift and drag forces while the distribution is more concentrated to the right of the mean value, with a minimum value of -1.872728 for angles of attack equal to 0, 5, and 45 degrees. For most angles ranging from 10 to 40 degrees, the distribution shifts towards positive values, with a maximum of 1.580017. The curve appears to be symmetric, with a skewness value of 0.446234, which is relatively low.

In cases of 0, 5, 15, 20, and 25 degrees, the Kurtosis values are positive, indicating that the distribution is Leptokurtic, unlike angles of 10, 40, and 45 degrees where the values are negative, indicating a Platykurtic distribution. Lastly, for cases where the angle of attack is 30 and 35 degrees, the values are close to zero, indicating a Mesokurtic distribution.

The SST Transient turbulent model is an extension of the SST k-Omega model, where, in addition to the two classic equations from the previous model, there is an additional transport equation. This allows for a turbulent model consisting of a total of three equations.

For the analysis of low-speed external flow over a spoiler or airfoil profile, the most suitable model for both low and high angles of attack is the k-ω model, where chaotic motion is calculated by solving two equations. Unlike the Spalart-Allmaras model, the k-ω model is more accurate and also suitable for low Reynolds number internal flows. This model is widely popular for automotive applications and, due to its low computational power requirements, it has an acceptable time-consuming process.

Conclusion

To perform the numerical analysis of a 3D cambered airfoil with a chord length of 10 cm and a span of 4 units, a finite volume-based software was used. This software allows for dividing the volume into very small cells and analyzing their movement to calculate aerodynamic forces such as lift and drag. The chosen airfoil profile was the NACA 6409, rotated 180 degrees as it is intended for automotive use to generate downforce. The high-cambered spoiler is capable of generating more downforce at near-zero angles of attack compared to a symmetric profile, which requires a higher angle of attack to generate significant downforce. The simulations were conducted at a velocity of 50 m/s, considering the fluid as incompressible and with a constant temperature of 20 degrees Celsius.

After creating the 3D airfoil profile, the reference domain was defined to allow the airflow to pass through with its corresponding boundary conditions. The mesh was refined near the surfaces of the spoiler to obtain accurate lift and drag results. The pressure and velocity vary depending on the turbulence numerical model used for angles of attack greater than 15 degrees when the stall effect occurs. Analyzing all the results of the turbulence models, the k-kL-Omega model, which uses three equations to solve turbulence, appears to be the most suitable for such conditions. This model closely approximates the mean value. For low angles of attack, the difference between turbulent models is not very noticeable, while for high angles of attack, the difference becomes more pronounced.

Observing the lift force graph for angles of attack below the stall point, the curves are close to the mean value, while for angles of attack greater than the stall point, the turbulent models diverge. From the analysis of the drag and lift results compared to the mean value, the SST K-Omega model proves to be the most suitable, consistent with other results obtained in other experiments. The SST K-Omega model fits well for such requirements as it does not require high computational power, and the results are fairly accurate in the case of external flows with low velocities. Additionally, being a hybrid model, it combines the advantages of both k-Omega and k-Epsilon models.

References

http://www.airfoiltools.com/

Saurabh B., Md. Zunaid, Naushad A. A., Sagar S., Rohit S. D. (2015). CFD Simulation of Flow around External Vehicle: Ahmed Body, PP 87-94, www.iosrjournals.org

Ahmed, H[aseeb] & Chacko, S[ibi] (2012). Computational Optimization of Vehicle Aerodynamics. Annals of DAAAM for 2012 & Proceedings of the 23rd International DAAAM Symposium, Volume 23

Vignesh S., Vikas S. G., Jishnu V., Maheswarreddy, Amal K., Yagna S. M., (2018). Windscreen angle and Hood inclination optimization for drag reduction in cars. 14th Global Congress on Manufacturing and Management (GCMM-2018). Procedia Manufacturing 30 (2019) 685 – 692

Rubel C. D., Mahmud R., (2017). CFD Analysis of Passenger Vehicle at Various Angle of Rear End Spoiler. 10th International Conference on Marine Technology, MARTEC 2016. Procedia Engineering 194 (2017) 160 – 165

McCormick, Barnes W. (1979). Aerodynamics, Aeronautics, and Flight Mechanics. p. 24, John Wiley & Sons, Inc., New York

Mohd. R., Ahmed W., (2017) Vol. 5 Issue 3, A Study on Airflow over a Car, International Journal of Science, Engineering and Technology

John D., Anderson Jr., (2011) Fundamentals of Aerodynamics, Fifth Edition, p. 77, 125

Anagha S Gowda, Comparison of Aerodynamic Performance of NACA 4412 and 2412 using Computational Approach, International Journal of Engineering Trends and Technology (IJETT) - Volume 67 Issue 4 - April 2019

An Introduction to Aircraft Structural Analysis by T. H. G. Megson, Elsevier Ltd., 2010

Pritchard, P. (2011). Fox and McDonald's Introduction to Fluid Mechanics (Eighth edition), John Wiley & Sons, ISBN-13 9780470547557, ISBN-10 0470547553, New York, NY.

Imran Ismail Sheikh, Numerical Investigation of Drag and Lift Coefficient on a Fixed Tilt Ground Mounted Photovoltaic Module System over Inclined Terrain, International Journal of Fluids Engineering. ISSN 0974-3138 Volume 11, Number 1 (2019), pp. 37-49

Mesh Quality & Advanced Topics of Introduction to ANSYS Meshing

S. Goyal, A. Kulshreshtha, S. Singh, Selection of Turbulence Model for Analysis of Airfoil Wing using CFD, International Research Journal of Engineering and Technology (IRJET), Volume: 08 Issue: 03, Mar 2021

Tuncay Kamas, 2-D and 3-D Assessment of Cambered and Symmetric Airfoils: A CFD Study, Clemson University

https://www.afs.enea.it/project/neptunius/docs/fluent/html/th/node71.htm